Desalination and Water Treatment
www.deswater.com
doi: 10.5004/dwt.2021.27174

224 (2021) 273–281
June

Adsorption of manganese ions from aqueous solution by using manganese oxide coated zeolite

Md. Wasikur Rahman[a,*], Huei Ruey Ong[b], Wendy Yin Jou Kong[b], Hamidah Abdullah[b], Md. Maksudur Rahman Khan[b]

[a] *Department of Chemical Engineering, Jashore University of Science and Technology, Jashore – 7408, Bangladesh, Tel. +88 0421 62020; Fax: +88 0421 61199; email: w.rahman@just.edu.bd/mwrahman.ump@gmail.com*
[b] *Department of Chemical Engineering, College of Engineering, University Malaysia Pahang, 26300 Gambang, Pahang, Malaysia, emails: oi_rui86@hotmail.com (H.R. Ong), wendy_4491@hotmail.com (W.Y.J. Kong), hamidah@ump.edu.my (H. Abdullah), mrkhancep@yahoo.com (M.R. Khan)*

Received 26 September 2020; Accepted 24 February 2021

ABSTRACT

Manganese oxide coated zeolite (MOCZ) has been demonstrated in the present issue as a potential adsorbent for the removal of manganese (Mn^{2+}) from Mn^{2+} containing aqueous solution by batch adsorption process. The adsorption capacity of the as-prepared MOCZ was determined over the parameters of contact time, adsorbent dosage, pH and Mn^{2+} concentration. Surface properties of the MOCZ were analyzed by Brunauer–Emmett–Teller, X-ray diffraction and field emission scanning electron microscopy. Results showed that MOCZ has a high degree of crystallinity and the surface of MOCZ is mainly vernadite (γMnO_2) with a specific surface area and average pore diameter of 39.9 $m^2 g^{-1}$ and 1.17 nm, respectively. Besides, the adsorption process was found to be strongly pH-dependent and Mn^{2+} adsorption increased with pH and adsorbent dosage. Adsorption kinetics of Mn^{2+}/MOCZ system followed pseudo-second-order model successfully and equilibrium data were fitted with isotherm models of Langmuir and modified Langmuir. As-proposed two sites one molecule adsorption mechanism fitted well with the equilibrium data and maximum adsorption capacity of Mn^{2+} was found to be 0.93 meq $Mn^{2+} g^{-1}$. Therefore, MOCZ can be employed as an effective and alternative to commercial adsorbents for the removal of manganese from an aqueous solution.

Keywords: Wastewater treatment; Adsorption; Manganese; Zeolite; Langmuir isotherm; Kinetics

1. Introduction

Nowadays the environmental pollution by heavy metals demonstrates the most critical concern worldwide. Various heavy metals are released from industries as effluents [1,2], typically from chemical process plants as well as mining, metal plating and finishing, rubber processing, etc. [3,4]. The maximum allowable discharge quantity of heavy metals is in a very minute amount. The maximum allowable level of Mn^{2+} contamination in drinkable water is <0.1 mg L^{-1} stated by World Health Organization (WHO) [5]. According to Malaysia Sewage and Industrial Effluent Discharge Standard [6], the manganese discharge limit in industrial sectors is 0.2 and 1.0 mg L^{-1} for standard A and B, respectively. There are huge contaminants released into the environment that are considered toxic chemicals.

---

* Corresponding author.

The toxicity of these elements is higher than the level defined by WHO and they may cause serious risks to human health and ecology [7]. It is said that "manganese does not present a danger to human health, nor for the environment but it is unpleasant". However, prolonged exposure of manganese to mankind may affect lung tissue and even the central nervous system [8]. Problems associated with the presence of manganese by influencing bacterial growth include laundering operation, plumbing fixtures and distribution systems [4]. By far, human suffers no harmful effects from drinking water that contains very trace amount of manganese. Nevertheless, uptake manganese from groundwater as it is a source of drinking water has become a challenge due to its much higher concentration in groundwater and highly reactive properties [9].

In order to remove heavy metals from wastewater, a number of methods are employed such as filtration, chemical precipitation, ion exchange, membrane separation, adsorption, etc. Most of the methods are inefficient at a very low concentration of heavy metals and relatively expensive [4]. In addition, these operations produce secondary effluent that has an adverse impact on the environment [10]. Adsorption, in particular, an alternative process that is more attractive than the other techniques as it is highly effective, economic, versatile and easy to operate [11]. Therefore, cost-effective adsorbents with high potentiality are the current demand for practical application to remove heavy metals from industrial wastewater.

Zeolites are the most commonly used adsorbents in the water treatment process. They are reactive crystalline solids chemically known as hydrated aluminosilicates having regular microporous structures [12]. Exchangeable cations of alkaline and alkaline earth metals (e.g., Na^+, K^+, Ca^{+2}, Mg^{+2}, etc.) are the basis of the structural framework of zeolites. They are interesting adsorbents owing to exciting surface area and cost-effective properties [13], however, their performance needs to be improved regarding adsorption capacity, tensile properties and resistance to chemicals. Therefore, a number of methods have been practiced to modify surface features of zeolites by physicochemical treatment [14]. Coating onto zeolites (e.g., MnO_2), for instance, is demonstrated as one of the most widespread applications [15].

Manganese(IV) oxide (MnO_2) is a porous material having a large surface area. It is a mild oxidant and chemically stable in acidic conditions [16]. Additionally, MnO_2 has the ability to form thin films and demonstrates mesoporous characteristics as an adsorbent [17]. Nevertheless, pure MnO_2 is not much interesting adsorbent as it is very difficult to separate from the aqueous phase and comparatively costly [15].

The objective of this research is to synthesize and characterize manganese oxide coated zeolite (MOCZ) as an adsorbent to remove manganese (Mn^{2+}) from an aqueous solution by the batch process. This manuscript also investigates the effect of contact time, adsorbent dosage and pH on the adsorption capacity. Moreover, adsorption kinetics and equilibrium isotherm of the system (Mn^{2+}/MOCZ) have been studied including modified Langmuir adsorption isotherm as proposed for the removal of manganese by MOCZ adsorbent.

2. Materials and methods

2.1. Materials and reagents

Zeolites employed in the synthesis of MOCZ were granular shapes. Chemical reagents such as $KMnO_4$, NaCl and HCl were used to synthesize MOCZ. Manganese(II) sulfate monohydrate ($MnSO_4{\cdot}H_2O$) was utilized as a source of manganese in the preparation of Mn^{2+} containing aqueous solution. Aqueous solutions of 0.1 M HCl and 0.1 M NaOH were used as per the requirement to adjust pH during adsorption. All chemicals were purchased from Sigma-Aldrich (Germany) and distilled water was used to prepare the solutions.

2.2. Synthesis of MOCZ

Zeolite sample has the chemical formula of $(Na, K, Ca)6(Si, Al)_{36}O_{72}{\cdot}20H_2O$ containing clinoptilolite (70 wt.%) collected from the local supplier. The zeolite was ground and sieved with a particle diameter of <149 μm. The zeolite was cleaned with distilled water several times to remove impurities from the sample. MOCZ was prepared by dissolving 30 g of zeolite sample in ½ L of 1 M NaCl solution for 24 h to convert it into Na form. The suspension of zeolite was then filtered and washed several times with deionized water followed by drying prior to use at 100°C for 24 h [9]. MOCZ was prepared by reduction reaction [18] and manganese(IV) oxide colloids were precipitated onto the Na-zeolite surfaces by the reaction (1):

$$2KMnO_4 + 8HCl = 2MnO_2\downarrow + 2KCl + 3Cl_2 + 4H_2O \tag{1}$$

Potassium permanganate solution ($KMnO_4$) heated at 100°C was poured over the Na-zeolite sample. Then an aqueous solution of HCl (37.5% w_{HCl}/w_{H_2O}) was added dropwise into the solution and stirred for 1 h. After that, the suspended material was successfully filtered and washed several times in order to discard free K^+ and Cl^- ions. The as-prepared sample was dried in the above conditions and stored for further use.

2.3. Characterization of MOCZ

Surface area and pore size analyzer were employed to detect surface properties and pore size distribution of MOCZ following N_2 adsorption method and Brunauer–Emmett–Teller (BET) adsorption model was used in the calculation of specific surface area and pore volume of the zeolite. The phase composition of the coated zeolite was determined by using X-ray diffraction (XRD) with a source of Cu Kα radiation. Morphological properties of MOCZ were investigated by field emission scanning electron microscopy (FESEM) (JEOL, JSM-7800F, Japan).

2.4. Adsorption experiments

The model solution was prepared by dissolving $MnSO_4{\cdot}H_2O$ in distilled water. The stock solution of Mn^{2+} (1 g L^{-1}) was prepared and working solutions of 50, 100, 150, and 200 mg L^{-1} were made by dilution method. Manganese ion concentration was estimated by flame atomic absorption spectroscopy (AAS) analyzer and the results were expressed in the unit of mg Mn^{2+} L^{-1}. Batch experiments were performed in a conical flask of 250 mL under constant agitation of 150 rpm. Supernatant aliquots were collected and centrifuged at 8,000 rpm for 10 min and filtered prior to analysis by AAS. Batch studies were done at different $MnSO_4{\cdot}H_2O$ solutions at a constant pH of 7 and contact time of 120 min. The initial concentration and pH were measured. 1 g of MOCZ was added into 100 mL of 50 mg Mn^{2+} L^{-1} solution and agitated for 120 min. At different time intervals, the supernatant aliquots were successively collected, centrifuged and filtered for further analysis. This procedure was repeated for 100, 150, and 200 mg L^{-1} of $MnSO_4{\cdot}H_2O$. Suspension of 1 g of MOCZ was added into 150 mg Mn^{2+} L^{-1} solution at initial pH of 7. The initial concentration of the solution was measured and the supernatant aliquots were collected and filtered after 120 min before analysis. The procedure was repeated by using an adsorbent dosage of 5 and 7 g, respectively in 150 mg Mn^{2+} L^{-1}.

3. Results and discussion

3.1. Characterization of MOCZ

Specific surface area and pore volume of the as-prepared MOCZ were estimated following the N_2 adsorption method and the BET adsorption model was used to determine the surface properties. The specific surface area of the MOCZ for adsorbed Mn^{2+} was found to be 39.90 m^2 g^{-1} after degassing at 300°C overnight. Zou et al. [14] revealed that owing to the coating of manganese(IV) oxide on the zeolite surface, its surface area increased from 24.87 to 28.23 m^2 g^{-1}; on the contrary, the average pore diameter of the Na-zeolite decreased from 28.66 to 26.72 Å. In fact, MOCZ does not have a high surface area as that compared to *Nypa fruticans* (112.29 m^2 g^{-1}), more expensive alternatives of activated carbon (1,688 m^2 g^{-1}) and carbon nanotubes (177 m^2 g^{-1}) [19]. However, this value is reasonably higher than that of the more expensive adsorbent of graphene oxide (32 m^2 g^{-1}) reported elsewhere [20]. Therefore, MOCZ can be proposed as an alternative to some selective cost-effective carbonaceous adsorbents.

The XRD pattern of the as-prepared MOCZ is demonstrated in Fig. 1 and mineral phases that exist in the sample are inserted in Table 1. The diffraction peaks of the zeolite match well with the peaks of the standard A-type zeolite (Fig. 1, inset) [21,22]. The degree of complexity of the zeolite is a function of surface area and degree of crystallinity of the crystal as shown in the XRD pattern. Various crystalline forms of the zeolite (Table 1) are the cause of the degree of complexity as well as responsible for higher surface properties and crystallinity. The diffractogram also represents that manganese(IV) oxide coated on the surface of the zeolite is known as vernadite ($MnO_2{\cdot}nH_2O$) and chemically denoted by γMnO_2 [23].

FESEM micrograph was taken into account to observe the surface morphology of as-prepared MOCZ with a magnification of 14,000 times (Fig. 2) and manganese oxides were possibly deposited on the surface as detected by XRD. The figure shows that surface sites of the zeolite were occupied by new-fangled MnO_2 species which were uniformly distributed, with no agglomeration of the metal oxides. In fact, small particles more precisely nanoparticles ameliorate surface features. Small components of the synthetic coating are distributed on the surface of the zeolite results in a more consolidated coating. Manganese(IV) oxide particles with a diameter of 1–3 μm appeared to be growing thru surface depressions and coating cracks. Moreover, the clusters of manganese oxides are formed onto the surface of the sodium-based zeolites that facilitate the adsorption process. Similar phenomena were also reported elsewhere [8,22,24].

Table 1
Major mineral phases exist in the as prepared MOCZ sample

Phases	Molecular formula	Peak nos.
Mordenite	$(Ca, Na_2, K_2)\ Al_2Si_{10}O_{24}{\cdot}7H_2O$	1,2
Clinoptilolite	$(Na, K, Ca)6(Si, Al)_{36}O_{72}{\cdot}20H_2O$	3
Vemadite	$MnO_2{\cdot}nH_2O$	4,5,7,8
Quartz	SiO_2	6

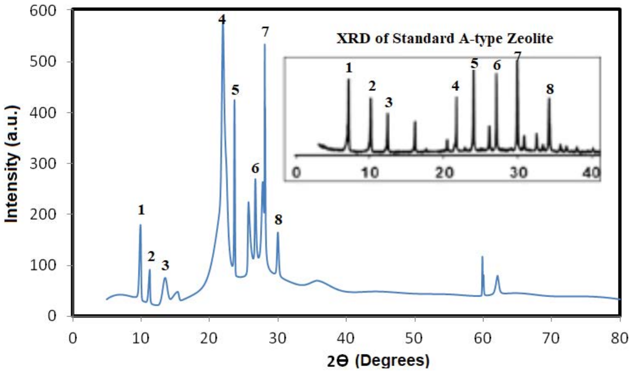

Fig. 1. XRD of as prepared MOCZ and standard A-type zeolite (inset).

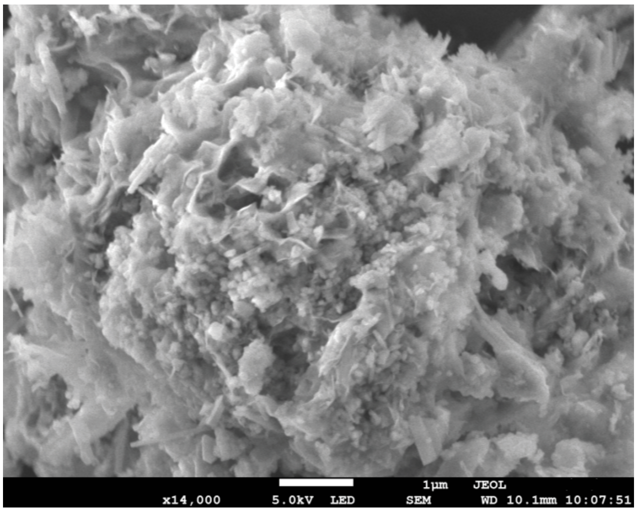

Fig. 2. FESEM image of as-prepared MOCZ with a magnification of 14,000 times.

3.2. *Effect of contact time on adsorption of MOCZ*

Adsorption capacity, q (mg g^{-1}) and the adsorption of Mn^{2+} at different concentrations and contact times are presented in Fig. 3. Initial concentrations of Mn^{2+} varied from 50 to 200 mg L^{-1}, the time needed to attain equilibrium was increased; in contrast, the Mn^{2+} removal was decreased from 90% to 55%. Moreover, the plot revealed that the amount of Mn^{2+} adsorbed increased while increasing the concentration. Manganese removal capacity of MOCZ adsorbent increased with an increase in Mn^{2+} ion concentration in the solution in order to available metal ions. Existing metal ion concentration is a function of mass transport between aqueous and solid phases. In fact, driving force increased with higher Mn^{2+} concentration to overcome mass transfer resistances of the metal ions point out that the probability of ionic collision of Mn^{2+}/MOCZ increased. This phenomenon also results in higher removal efficiency of metal ions through adsorption [25].

3.3. *Effect of MOCZ dosage*

The relationship between the amount of Mn^{2+} adsorbed on MOCZ and the adsorbent dosage is shown in Fig. 4. From the graph, the removal of manganese increased while increasing the dosage of MOCZ adsorbent from 1 to 7 g L^{-1} and maximum recovery of Mn^{2+} was obtained to be 70.32% for 7 g L^{-1} dosages. The reason behind high uptake capacity may be a greater amount of MOCZ adsorbent results in the available surface area [26,27] and hence more active sites present in the system.

3.4. *Effect of pH*

pH of a solution plays a vital role in the removal of Mn^{2+} using MOCZ adsorbent. Adsorption of Mn^{2+} ions enhanced with pH increased from 4 to 8 by using an aqueous solution of Mn^{2+} (150 mg L^{-1}) (Fig. 5). Inhibition of Mn^{2+} removal was possibly observed at lower pH owing to the competition between H^+ and Mn^{2+} ions for mass transfer on exchangeable surface sites with the dominance of H^+ ions. Negative charge density on the adsorbent surface increased with pH might be due to deprotonation of metal-binding sites results in enhancement of Mn^{2+} adsorption. The adsorption mechanism of the system can be explained by the ion exchange reaction where Mn^{2+} ions adsorbed onto MOCZ as well as Mn^{2+} exchanged with H^+ ions on the surface results in the formation of a surface complex confirmed by the XRD experiment. The surface reaction of the divalent ions with metal oxide surfaces has been reported elsewhere [28–31]. The main interactions are summarized as follows:

- Free metal ions (X^{2+}) associated with surface hydroxyl groups (OH^-) (ion exchange with H^+ ions)

$$\equiv \mathrm{MnOH} + \mathrm{X}^{2+} \leftrightarrow \mathrm{MnOX}^{+} + \mathrm{H}^{+} \tag{2}$$

- Formation of hydrolysis complex and adsorption

$$\equiv \mathrm{MnOH} + \mathrm{X}^{2+} + \mathrm{H_2O} \leftrightarrow \mathrm{MnOXOH} + 2\mathrm{H}^{+} \tag{3}$$

- Bidendate complex formation

$$2(\equiv \mathrm{MnOH}) + \mathrm{X}^{2+} \leftrightarrow (\equiv \mathrm{MnO})_2\,\mathrm{X} + 2\mathrm{H}^{+} \tag{4}$$

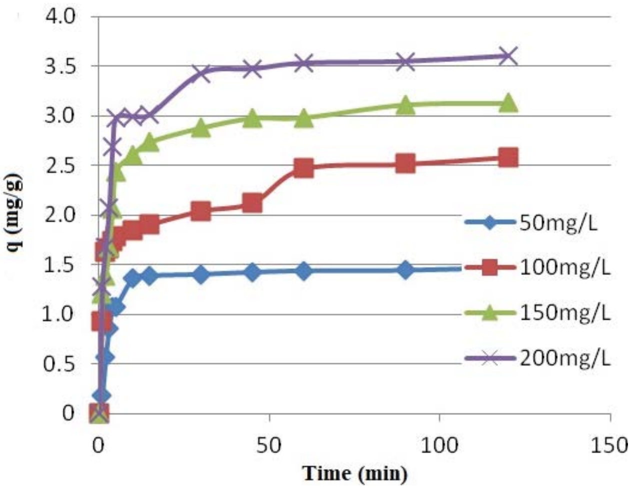

Fig. 3. Plot of the steady values of Mn^{2+} adsorbed vs. contact times with different initial concentrations at initial pH 7 and dose 1 g of MOCZ.

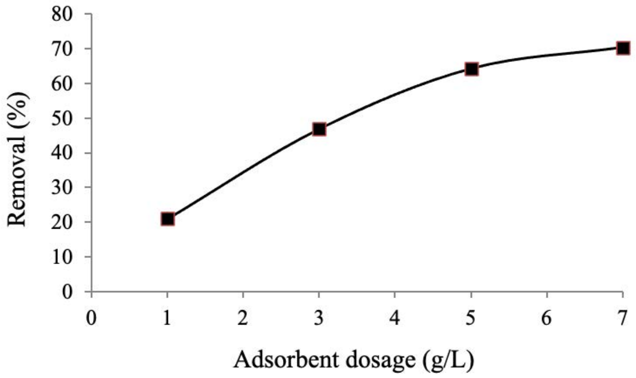

Fig. 4. Plot showing the effect of MOCZ adsorbent dosage for Mn^{2+} removal at initial concentration 150 mg L^{-1} and pH 7.

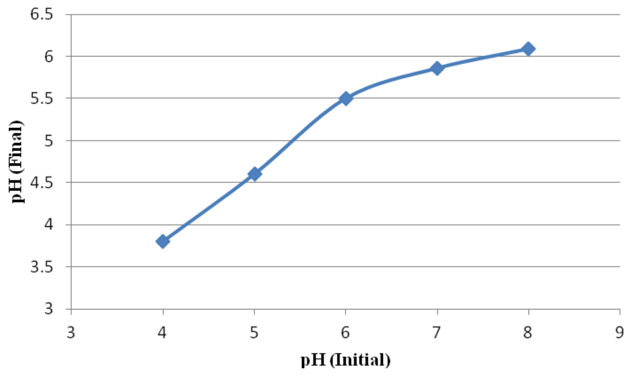

Fig. 5. Plot presenting the relationship between initial pH and final pH values during adsorption of Mn^{2+} at an initial concentration of 150 mg L^{-1} and dose 1 g of MOCZ.

Rendering to the reaction schemes, Mn^{2+} ions are possibly adsorbed onto the MOCZ adsorbent and H^+ ions are released in parallel which ultimately reduces pH values. As released two H^+ ions adsorbed for each Mn^{2+} ion suggest the complex formation of either hydrolysis or bidendate reaction shown in Fig. 6. The concentration of manganese species at different pH values were calculated and plotted in the figure. Table 2 shows different concentrations of manganese with equilibrium constants.

Manganese species, in particular, Mn^{2+} ions are predominantly adsorbed on MOCZ surface at lower pH detected by final pH value (Fig. 5) which is almost constant up to pH 7.5. Manganese species are generally adsorbed in the complex form and hydrolysis complex formation $[Mn(OH)]^+$ increases with an increase in pH. Fig. 6 shows that for pH > 7.5, the change in final pH is higher and the concentration of adsorbed Mn^{2+} ions and $[Mn(OH)]^+$ complex is roughly in equality; thus concentrations of [≡MnOXOH] and $[\equiv MnOX^+]$ would be the same.

It is evident from the experiment that solution pH deviated from 7 hampered the adsorption process. The MOCZ adsorbent is protonated in an acidic medium. The removal efficiency of manganese is greatly decreased while protons (H^+) and Mn^{2+} are competing in order to binding on reactive sites; however, Mn^{2+} ions demonstrate the repulsive effect on the positively charged surface. Almost similar results were also reported in [36] point out that uptake efficiency of activated carbon was decreased owing to high interference of protons which ultimately damage the adsorbent. At pH > 7, there is a possibility of the electrostatic repulsion between Mn^{2+} species and adsorbent surface with negative charges decreased the rate of metal removal. In fact, the number of hydroxyl groups (OH^-) increases with an increase in solution pH; thus, the number of positively charged sites decreases and the attraction between Mn^{2+} ions and MOCZ surface reduces. Moreover, at higher pH (pH > 7) Mn species maybe interact with OH^- to form manganese hydrous oxide $[Mn(OH)]^+$ that shows sluggish kinetics of Mn adsorption in the system [37].

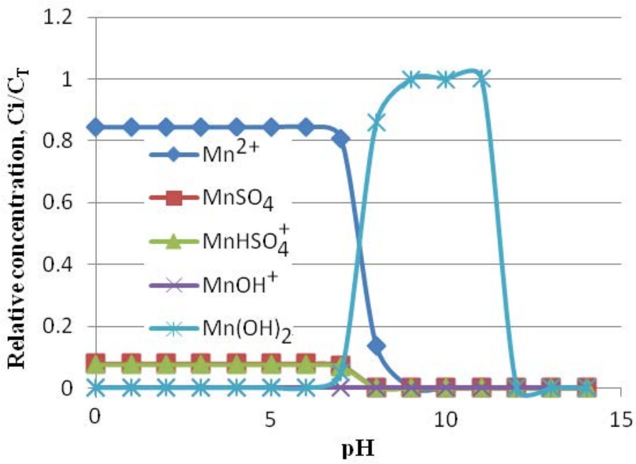

Fig. 6. Plot of the relative concentration of different manganese species with pH at an initial concentration of 0.592 mmol L^{-1} and dose 1 g of MOCZ.

Table 2
Chemical reaction equilibrium constants (k_1) for manganese species

Chemical reaction	k_1	References
$Mn^{2+} + SO_4^{2-} = MnSO_4$	190	[32]
$Mn^{2+} + HSO_4^- = MnHSO_4^+$	181.97	[33]
$Mn^{2+} + OH^- = MnOH^+$	6.27×10^3	[34]
$Mn^{2+} + 2OH^- = Mn(OH)_2$	6.31×10^{12}	[35]

3.5. Adsorption isotherm

Basic parameters of the separation technique are considered to be adsorption isotherms [38] and adsorbent capacity is determined from the linear fitting of the equilibrium data. The equation of the Langmuir model is employed, in general, for the study of the adsorption isotherms at a constant temperature to develop a design model of wastewater treatment.

The concept of monolayer formation on the adsorbent surface with ideal sites of uniform energies without transmigration of adsorbate molecules in the bulk can be explained by the Langmuir isotherm model. The following equation represents the isotherm model for the solid–liquid system:

$$\frac{1}{q} = \frac{1}{kq_{\max}} \frac{1}{C_e} + \frac{1}{q_{\max}} \tag{5}$$

where Langmuir parameters, $q_{\max}$ is the maximum adsorption capacity (mg g^{-1}) for monolayer formation at equilibrium concentrations and K is the Langmuir isotherm constant (L mg^{-1}) [38].

The important properties of the Langmuir model can be, in general, described by a dimensionless quantity, R_L at equilibrium as follows:

$$R_L = \frac{1}{\left(1 + KC_0\right)} \tag{6}$$

where K defined earlier indicates the nature of adsorption and initial concentration of Mn^{2+} (mg L^{-1}) is indicated as C_0. R_L directs the types of isotherm of the system as $R_L > 1$: unfavorable, $R_L = 1$: linear as well as $0 < R_L < 1$: favorable and $R_L = 0$: irreversible. Based on Eq. (6), R_L value is 9×10^{-5}, indicating the favorable conditions for Mn^{2+} adsorption.

3.6. Adsorption kinetics

Adsorption kinetics was evaluated by two different models: (1) pseudo-first-order [39] and (2) pseudo-second-order kinetic model [40] and corresponding experimental results are presented in Table 3. The Lagergren first-order model is based on the manganese uptake capacity for the liquid/solid adsorption system. The linear form of the equation is expressed as perfect correct:

$$\log\left(q_e - q_t\right) = \log\left(q_e\right) - \frac{k_1}{2.303} t \tag{7}$$

Table 3
Kinetic parameters of pseudo-first and second-order models evaluated for Mn^{2+} ions adsorbed onto MOCZ

Pseudo-first-order model				Pseudo-second-order model		
$q_{e,\text{exp.}}$		$q_{e,\text{theor.}}$			$q_{e,\text{theor.}}$	
mg g^{-1}	k_1	(meq g^{-1})	R^2	k_1	(meq g^{-1})	R^2
29.80	19.81	33.99	0.948	152.89	0.0036	0.999

where q_e is the amount of heavy metal ion adsorbed (mg g^{-1}) at equilibrium, q_t is the amount adsorbed (mg g^{-1}) at time t, and k_1 is the Lagergren pseudo-first-order adsorption rate constant (min^{-1}).

The kinetic model of second-order reaction can be explained by the amount of adsorbate molecules is captured on the adsorbent surface. The kinetic rate of the adsorption process suggests a second-order mechanism and the rate equation can be expressed as:

$$\frac{t}{q_t} = \frac{1}{k_2 q_e^2} + \frac{1}{q_e} t \tag{8}$$

The adsorption process Mn^{2+}/MOCZ did not properly follow a pseudo-first-order reaction ($R^2 = 0.948$) as indicated in Table 3. The adsorption capacity (q_e) of the MOCZ adsorbent extracted from the kinetic model was not satisfactory in comparison to that of the experimental values (29.8 mg g^{-1}).

The adsorption process is properly associated with a pseudo-second-order kinetic model verified by correlation coefficient ($R^2 > 0.99$). The theoretical values of adsorption capacity (q_e) of MOCZ are strongly correlated to the values of experimental results. In fact, chemical adsorption can be defined by the rate-limiting step as one of the assumptions of this model where valence forces are involved over the exchange or sharing of electrons between adsorbent and adsorbate of the process [41].

Kinetic results for adsorption of Mn^{2+}/MOCZ system are illustrated in Fig. 7 where experimental outcomes were compared to those of theoretical data. It can be concluded that the experimental data did not fit well with the Langmuir model as the initial rate of adsorption is too high. Therefore, two sites one molecule mechanism were studied. One molecule would occupy two sites of adsorbent as demonstrated in this mechanism quite successfully.

3.7. Modified Langmuir model

Langmuir model of adsorption isotherm study has been proposed to be modified for two sites (B and S) one molecule (BS_2) type of adsorption can be defined as dual sites mechanism. The reaction schemes and equations become:

$$B + 2S \underset{k_2}{\overset{k_1}{\Leftrightarrow}} BS_2 \tag{9}$$

According to this sorption phenomenon, it is required two sites (B and S) fit one molecule (S_2B). So, the number of active sites is double to the number of molecules adsorbed. Thus:

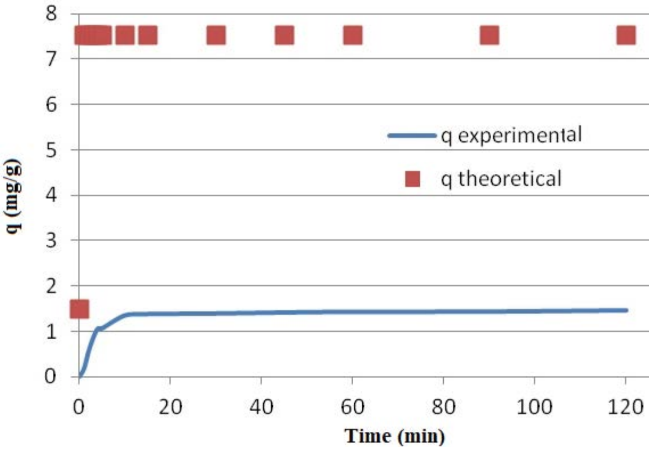

Fig. 7. Plot comparing theoretical and experimental quantities of Mn^{2+} adsorbed at an initial concentration of 50 mg L^{-1}, dose 1 g of MOCZ and initial pH 7.

$$C_{S_0} = \frac{2q_\infty w}{v} \tag{10}$$

$$C_{S_2B} = \frac{2qw}{v} \tag{11}$$

$$K = \frac{k_1}{k_2} = \frac{C_{S_2B}}{C_B C_S^2} \tag{12}$$

$$K = \frac{C_{S_2B}}{C_B \left(C_{S_0} - C_{S_2B}\right)^2} \tag{13}$$

$$KC_B = \frac{w}{2v} \frac{q}{\left(q_\infty - q\right)^2} \tag{14}$$

where C_{S_0}, C_B and C_{S_2B} correspond to initial concentration of reactant S; concentration of reactant B and concentration of product S_2B (mg L^{-1}) at the time, t; K is the Langmuir isotherm constant (L mg^{-1}) and the rest of the Langmuir parameters stands common meaning.

The rate of changes of occupied sites:

$$\frac{dC_{S_2B}}{dt} = k_1 C_B C_S^2 - k_2 C_{S_2B} \tag{15}$$

$$C_S = C_{S_0} - C_{S_2B} \tag{16}$$

Therefore, the kinetic model for two sites one molecules is shown as below:

$$\frac{dq}{dt} = k_1 C_B \frac{2w}{v} \left(q_\infty - q\right)^2 - k_2 q \tag{17}$$

The equilibrium data were fitted using the equations below:

$$q = q_\infty - \sqrt{\frac{w}{2Kv}}\sqrt{\frac{q}{C_B}} \tag{18}$$

Table 4 indicates that equilibrium and kinetic adsorption parameters, R^2 values for diverse systems considering different mechanisms. The theoretical values for Langmuir and two sites one molecule mechanisms were calculated. These calculated values are plotted against the corresponding time, *t* and the resulted curves were compared to the experimental values against the *t* curve. The values of experimental and theoretical results are shown in Figs. 8 and 9 corresponding to Langmuir model ($R^2 = 0.8147$) and two site one molecule (dual sites) ($R^2 = 0.998$) fittings.

In the adsorption of Mn^{2+} on MOCZ, the two isotherm models, for example, Langmuir and two sites one molecule models are applicable and the curves for the system at an initial concentration of 50 mg L^{-1} are presented in Fig. 10. It can be comprehended from the tentative outcomes that the fitting of the Langmuir model did not match well with the data (Fig. 10a); however, the modified Langmuir model, that is, the two sites one molecule model satisfied them quite properly (Fig. 10b). Similar findings were also reported in the literature where zeolites are employed for the removal of manganese from aqueous solutions [22,24,42]. It can be concluded that the adsorption of Mn^{2+} using MOCZ followed the two sites one molecule mechanism where one molecule will occupy two sites of the adsorbent.

Table 4
Equilibrium and kinetic adsorption parameters evaluated for MOCZ considering Langmuir and dual site mechanism

Mechanism	Equilibrium			Kinetic	
	K	$q_{\max}$	R^2	k_1	k_2
Langmuir	214.96	0.00693	0.8147	461 ± 39	5.064 ± 1
Dual sites	1,955.97	0.9267	0.998	0.0027	1.39×10^{-6}

The values of standard deviations from the experimental values for all the plots were calculated. The values of standard deviations for the Langmuir model and two sites one molecules mechanism were 0.03372 and 0.0001, respectively. It can be resolved that due to the smaller value of standard deviation; two sites one molecule mechanism is more applicable for this system.

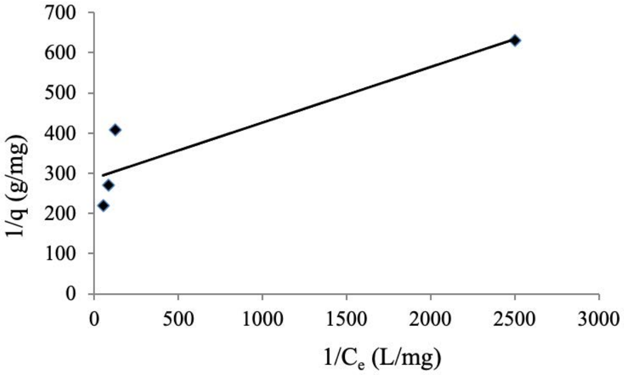

Fig. 8. Linear fitting of Langmuir adsorption isotherm.

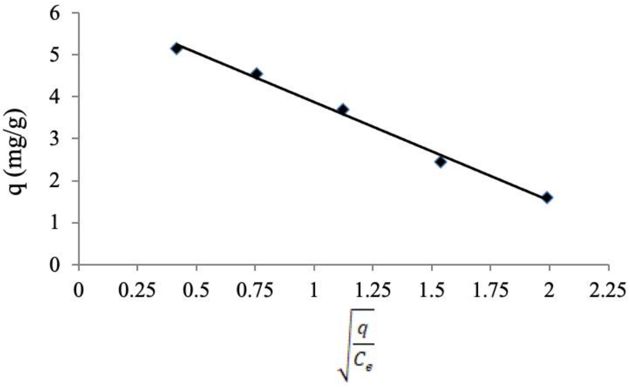

Fig. 9. Linear fitting of two sites one molecule adsorption isotherm.

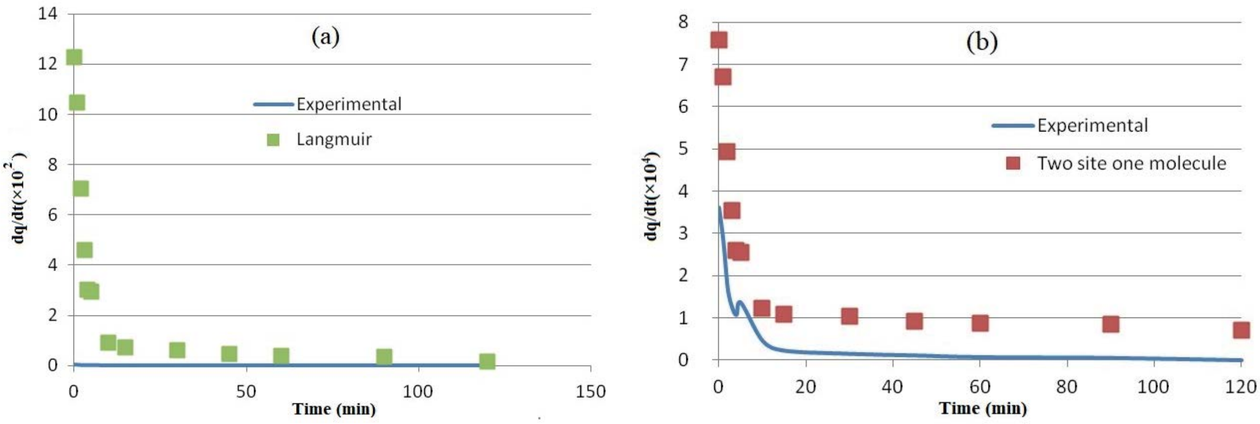

Fig. 10. Experimental and theoretical data presented by considering two different mechanisms at initial concentration 50 mg L^{-1}, dose 1 g of MOCZ and initial pH 7 (a) Langmuir model and (b) two sites one molecule.

4. Conclusion

The current study successfully demonstrates Mn^{2+} adsorption by MOCZ from contaminated water. The as-prepared MOCZ has high crystallinity and the oxide coating mainly presents as vernadite (γMnO_2) with a specific surface area of 39.9 $m^2 g^{-1}$ and an average pore diameter of 1.1733 nm. Results showed that the adsorption process of Mn^{2+}/MOCZ is a function of pH and Mn^{2+} adsorption increased with pH. The adsorption kinetics of the Mn^{2+}/MOCZ system followed pseudo-second-order kinetic model point out that the separation system may be chemical adsorption. Furthermore, the modified Langmuir model, that is, two sites one molecule model fitted well with equilibrium data, demonstrating high adsorption capacity of MOCZ for Mn^{2+} removal and the maximum capacity was found to be 0.9267 meq $Mn^{2+} g^{-1}$. Manganese uptake results in the combination of several interfacial reactive methods, for example, ion exchange, physisorption, chemisorption, reverse osmosis, etc. It can be proposed that the modified zeolite (MOCZ) would be an effective adsorbent for the removal of heavy metals from industrial wastewater.

Funding

The authors acknowledge the financial support from the Faculty of Chemical and Natural Resources Engineering, Universiti Malaysia Pahang.

References

[1] Z. Al-Qodah, Biosorption of heavy metal ions from aqueous solutions by activated sludge, Desalination, 196 (2006) 164–176.

[2] Z. Al-Qodah, M.A. Yahya, M. Al-Shannag, On the performance of bioadsorption processes for heavy metal ions removal by low-cost agricultural and natural by-products bioadsorbent: a review, Desal. Water Treat., 85 (2017) 339–357.

[3] B. Southichak, K. Nakano, M. Nomura, N. Chiba, O. Nishimura, *Phragmites australis*: a novel biosorbent for the removal of heavy metals from aqueous solution, Water Res., 40 (2006) 2295–2302.

[4] A.A. Mengistie, T. Siva Rao, A.V. Prasada Rao, Adsorption of Mn(II) ions from wastewater using activated carbon obtained from Birbira (*Militia ferruginea*) leaves, Global J. Sci. Front. Res. Chem., 12 (2012) 1–12.

[5] WHO, Guidelines for Drinking Water Quality. Health Criteria and Other Support Information, World Health Organization, 1996, pp. 248–253.

[6] K.Y. Tiller, Heavy Metals in Soils and Their Environmental Significance, B.A. Stewart, Ed., Advances in Soil Science, Vol. 9, Springer, New York, NY, 1989, pp. 113–142.

[7] D.C. Sharma, C.F. Forster, A preliminary examination into the adsorption of hexavalent chromium using low-cost adsorbents, Bioresour. Technol., 47 (1994) 257–264.

[8] S.R. Taffarel, J. Rubio, Removal of Mn^{2+} from aqueous solution by manganese oxide coated zeolite, Miner. Eng., 23 (2010) 1131–1138.

[9] Malaysia Sewage and Industrial Effluent Discharge Standards: Environmental Quality (Sewage and Industrial Effluents) (Amendment) Regulations 1997, Kuala Lumpur, Malaysia, 2020.

[10] F.L. Fu, Q. Wang, Removal of heavy metal ions from wastewaters: a review, J. Environ. Manage., 92 (2011) 407–418.

[11] Z. Zhu, C. Gao, Y.L. Wu, L.F. Sun, X.L. Huang, W. Ran, Q.R. Shen, Removal of heavy metals from aqueous solution by lipopeptides and lipopeptides modified Na-montmorillonite, Bioresour. Technol., 147 (2013) 378–386.

[12] I. Kuźniarska-Biernacka, A.M. Fonseca, I.C. Neves, Manganese complexes with triazenido ligands encapsulated in NaY zeolite as heterogeneous catalysts, Inorg. Chim. Acta, 394 (2013) 591–597.

[13] S.Q. Kong, Y.X. Wang, H.B. Zhan, S.H. Yuan, M. Yu, M.L. Liu, Adsorption/oxidation of arsenic in groundwater by nanoscale Fe-Mn binary oxides loaded on zeolite, Water Environ. Res., 86 (2014) 147–155.

[14] W.H. Zou, R.P. Han, Z.Z. Chen, J.H. Zhang, J. Shi, Kinetic study of adsorption of Cu(II) and Pb(II) from aqueous solutions using manganese oxide coated zeolite in batch mode, Colloids Surf., A, 279 (2006) 238–246.

[15] R.P. Han, W.H. Zou, Y. Wang, L. Zhu, Removal of uranium(VI) from aqueous solutions by manganese oxide coated zeolite: discussion of adsorption isotherms and pH effect, J. Environ. Radioact., 93 (2007) 127–143.

[16] J.W. Murray, The surface chemistry of hydrous manganese dioxide, J. Colloid Interface Sci., 46 (1974) 357–371.

[17] Z.W. Zhao, J. Liu, F.Y. Cui, H. Feng, L.L. Zhang, One pot synthesis of tunable Fe_3O_4–MnO_2 core-shell nanoplates and their applications for water purification, J. Mater. Chem., 22 (2012) 9052–9057.

[18] M. Richter, H. Berndt, R. Eckelt, M. Schneider, R. Fricke, Zeolite-mediated removal of NO_x by NH_3 from exhaust streams at low temperatures, Catal. Today, 54 (1999) 531–545.

[19] M.Y. Ali, M.W. Rahman, M. Moniruzzaman, M.J. Alam, I. Saha, M.A. Halim, A. Deb, M.S.A. Sumi, S. Parvin, B.K. Biswas, M.A. Haque, M.R. Khan, M. Khan, *Nypa fruticans* as a Potential Low-cost Adsorbent to Uptake Heavy Metals from Industrial Wastewater, Vol. 55, Conference of Engineering & Technology, Computer, Basic & Applied Sciences (ECBA 2016), Singapore, 25–26 January 2016, pp. 18–25.

[20] M.M.R. Khan, M.W. Rahman, H.R. Ong, A.B. Ismail, C.K. Cheng, Tea dust as a potential low-cost adsorbent for the removal of crystal violet from aqueous solution, Desal. Water Treat., 57 (2016) 14728–14738.

[21] M.K. Seliem, S. Komarneni, Equilibrium and kinetic studies for adsorption of iron from aqueous solution by synthetic Na-A zeolites: statistical modeling and optimization, Microporous Mesoporous Mater., 228 (2016) 266–274.

[22] A.M. Zayed, A.Q. Selim, E.A. Mohamed, M.S.M. Abdel Wahed, M.K. Seliem, M. Sillanpää, Adsorption characteristics of Na-A zeolites synthesized from Egyptian kaolinite for manganese in aqueous solutions: response surface modeling and optimization, Appl. Clay Sci., 140 (2017) 17–24.

[23] L.S. Balistrieri, J.W. Murray, The surface chemistry of δMnO_2 in major ion seawater, Geochim. Cosmochim. Acta, 46 (1982) 1041–1052.

[24] M.I.S. de Mello, E.V. Sobrinho, V.L.S.T. da Silva, S.B.C. Pergher, V or Mn zeolite catalysts for the oxidative desulfurization of diesel fractions using dibenzothiophene as a probe molecule: preliminary study, J. Mol. Catal., 482 (2020) 100495, doi: 10.1016/j.mcat.2018.02.009.

[25] S. Mandina, F. Chigondo, M. Shumba, B.C. Nyamunda, E. Sebata, Removal of chromium(VI) from aqueous solution using chemically modified orange (*Citrus cinensis*) peel, J. Appl. Chem., 6 (2013) 66–75.

[26] M.W. Rahman, M.Y. Ali, I. Saha, M. Al Raihan, M. Moniruzzaman, M.J. Alam, A. Deb, M.M.R. Khan, Date palm fiber as a potential low-cost adsorbent to uptake chromium(VI) from industrial wastewater, Desal. Water Treat., 88 (2017) 169–178.

[27] S. Parvin, M.W. Rahman, I. Saha, M.J. Alam, M.M.R. Khan, Coconut tree bark as a potential low-cost adsorbent for the removal of methylene blue from wastewater, Desal. Water Treat., 146 (2019) 385–392.

[28] H. Hohl, W. Stumn, Interaction of Pb^{2+} with hydrous C-Al_2O_2, J. Colloid Interface Sci., 55 (1976) 281–288.

[29] M.M. Benjamin, J.O. Leckie, Multiple-site adsorption of Cd, Cu, Zn, and Pb on amorphous iron oxyhydroxide, J. Colloid Interface Sci., 79 (1981) 209–221.

[30] Y.N. Chen, Y.Q. Liu, Y.P. Li, Y.X. Wu, Y.R. Chen, Y.H. Liu, J.C. Zhang, F.T. Xu, M.L. Li, L.S. Li, Synthesis, application and mechanisms of Ferro-Manganese binary oxide in water

remediation: a review, Chem. Eng. J., 388 (2020) 124313, doi: 10.1016/j.cej.2020.124313.

[31] R.P. Han, W.H. Zou, Z.P. Zhang, J. Shi, J.J. Yang, Removal of copper(II) and lead(II) from aqueous solution by manganese oxide coated sand: I. Characterization and kinetic study, J. Hazard. Mater. B, 137 (2006) 384–395.

[32] J. Bjerrum, G. Schwarzenbach, I.G. Sillen, Stability Constants of Metal Ion Complexes, Part II, Special Publ. 7, The Chemical Society, London, UK, 1958, pp. 131.

[33] R.M. Smith, A.F. Martell, Critically Stability Constants, Plenum Press, 1982, pp. 79–84.

[34] E.L. Shock, D.C. Sassani, M. Willis, D.A. Sverjensky, Inorganic species in geologic fluids: correlations among standard molal thermodynamic properties of aqueous ions and hydroxide complexes, Geochim. Cosmochim. Acta, 61 (1997) 907–950.

[35] Landolt-Bornstein, Thermodynamics Equilibria of the Extraction of Cobalt(II) from Scientific Group Thermodata Europe (SGTE), Springer Verlag, Berlin-Heidelberg, Germany, 1999, p. 405.

[36] H.R. Pouretedal, N. Sadegh, Effective removal of Amoxicillin, Cephalexin, Tetracycline and Penicillin G from aqueous solutions using activated carbon nanoparticles prepared from vine wood, J. Water Process Eng., 1 (2014) 64–73.

[37] S. Saha, A. Pal, Microporous assembly of MnO_2 nanosheets for malachite green degradation, Sep. Sci. Technol., 134 (2014) 26–36.

[38] R. Perry, D. Green, Perry's Chemical Engineers' Handbook, 7th ed., McGraw-Hill, New York, USA, 1999.

[39] S. Lagergren, Zur Theorie der sogenannten adsorption gelöster stoff, Kungliga Svenska Vetenskapasakademiens, Handlingar, 24 (1989) 1–39.

[40] G. McKay, The adsorption of basic dye onto silica from aqueous solution-solid diffusion model, Chem. Eng. Sci., 39 (1984) 129–138.

[41] V.C. Taty-Costodes, H. Fauduet, C. Porte, A. Delacroix, Removal of Cd(II) and Pb(II) ions, from aqueous solutions by adsorption onto sawdust of *Pinus sylvestris*, J. Hazard. Mater., 105 (2003) 121–142.

[42] M.R. Samarghandi, T.J. Al-Musawi, A. Mohseni-Bandpi, M. Zarrabi, Adsorption of cephalexin from aqueous solution using natural zeolite and zeolite coated with manganese oxide nanoparticles, J. Mol. Liq., 211 (2015) 431–441.